Physica D 238 (2009) 666–676

Contents lists available at ScienceDirect

Physica D

journal homepage: www.elsevier.com/locate/physd

Highly nonlinear solitary waves in heterogeneous periodic granular media

Mason A. Porter [a], Chiara Daraio [b,*], Ivan Szelengowicz [b], Eric B. Herbold [c], P.G. Kevrekidis [d]

[a] Oxford Centre for Industrial and Applied Mathematics, Mathematical Institute, University of Oxford, OX1 3LB, United Kingdom
[b] Graduate Aerospace Laboratories (GALCIT) and Department of Applied Physics, California Institute of Technology, Pasadena, CA 91125, USA
[c] Department of Mechanical and Aerospace Engineering, University of California at San Diego, La Jolla, CA 92093-0411, USA
[d] Department of Mathematics and Statistics, University of Massachusetts, Amherst, MA 01003-4515, USA

ARTICLE INFO

Article history:
Received 20 December 2007
Received in revised form
22 October 2008
Accepted 17 December 2008
Available online 3 January 2009
Communicated by R.P. Behringer

PACS:
05.45.Yv
43.25.+y
45.70.-n
46.40.Cd

Keywords:
Nonlinear waves
Solitary waves
Granular media
Lattices

ABSTRACT

We use experiments, numerical simulations, and theoretical analysis to investigate the propagation of highly nonlinear solitary waves in periodic arrangements of dimer (two-mass) and trimer (three-mass) cell structures in one-dimensional granular lattices. To vary the composition of the fundamental periodic units in the granular chains, we utilize beads of different materials (stainless steel, brass, glass, nylon, polytetrafluoroethylene, and rubber). This selection allows us to tailor the response of the system based on the masses, Poisson ratios, and elastic moduli of the components. For example, we examine dimer configurations with two types of heavy particles, two types of light particles, and alternating light and heavy particles. Employing a model with Hertzian interactions between adjacent beads, we find good agreement between experiments and numerical simulations. We also find good agreement between these results and a theoretical analysis of the model in the long-wavelength regime that we derive for heterogeneous environments (dimer chains) and general bead interactions. Our analysis encompasses previously-studied examples as special cases and also provides key insights on the influence of heterogeneous lattices on the properties (width and propagation speed) of the nonlinear wave solutions of this system.

1. Introduction

Ever since the Fermi–Pasta–Ulam problem was first investigated over a half a century ago, nonlinear oscillator chains have received a great deal of attention [1–4]. Over the past few years, in particular, chains of nonlinear oscillators have proven to be important in numerous areas of physics — including Bose–Einstein condensation in optical lattices in atomic physics [5–7], coupled waveguide arrays and photorefractive crystals in nonlinear optics [8,9], and DNA double-strand dynamics in biophysics [10].

The role of "heterogeneous" versus "uniform" lattices and the interplay between nonlinearity and periodicity has been among the key themes in investigations of lattice chains [11]. Here we investigate this idea using one-dimensional (1D) lattices of granular materials, which consist of chains of interacting spherical particles that deform elastically when they collide. The highly nonlinear dynamic response of such lattices has been the subject of considerable attention from the scientific community [12–28]. In contrast to traditionally-studied nonlinear oscillator chains, these systems possess a "double" nonlinearity that arises from the nonlinear contact interaction between the particles and a zero tensile response. This results in an asymmetric potential, which has in turn led to the observation of several new phenomena. In particular, some of the most interesting dynamic properties of such highly nonlinear systems appear for materials under precompression [12–15], at the interface between two different highly nonlinear structures [17,18,22,23], or at the interface between linear and nonlinear structures [24]. This completely new type of wave dynamics opens the door for exciting, fundamental physical insights and has the potential to ultimately yield numerous new devices and materials. Because granular lattices can be created from numerous material types and sizes, their properties are extremely tunable [12–15]. Furthermore, the addition of a static precompressive force can substantially vary the response of such systems and allows the selection of the wave's regime of propagation between highly nonlinear and weakly nonlinear dynamics [29]. Such tunability is valuable not only for studies of the basic physics of granular lattices but also in potential engineering applications. Proposed uses include shock and energy absorbing layers [18,23,25,26], sound focusing devices (tunable acoustic lenses and delay lines), sound absorption layers, sound scramblers [16,17,28], and more.

* Corresponding author. Tel.: +1 626 395 4479; fax: +1 626 449 6359.
E-mail address: daraio@caltech.edu (C. Daraio).

0167-2789/$ – see front matter © 2009 Elsevier B.V. All rights reserved.
doi:10.1016/j.physd.2008.12.010

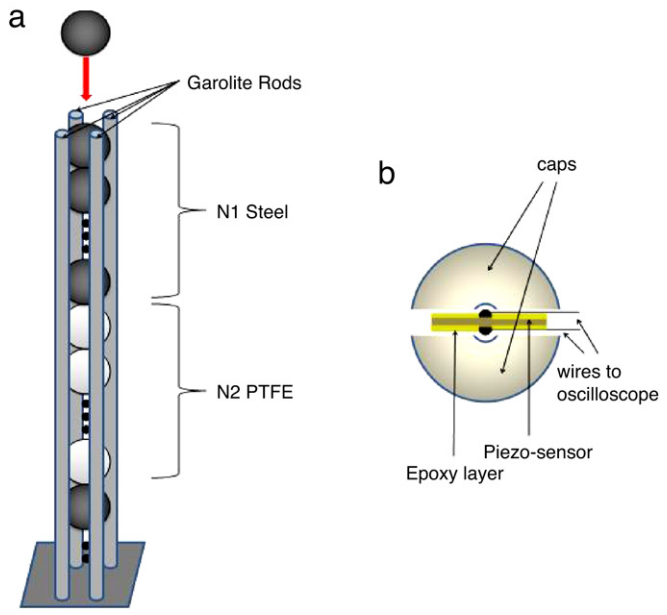

Fig. 1. (Color online) (a) Experimental setup for a dimer chain consisting of a periodic array of cells with N_1 consecutive beads of one material (e.g., stainless steel) and N_2 consecutive beads of another material (e.g., PTFE). (b) Schematic diagram of the composition of the sensors placed in the chain.

In the present work, we focus on one of the fundamental physical properties of such chains. Namely, because they are highly nonlinear, granular lattices admit a novel type of wave solution whose qualitative properties differ markedly from those in weakly nonlinear systems. Indeed, it was the experimental realization of such waves and the theory developed for uniform lattice systems of this type that has motivated the current broad interest in such settings [12,13]. The remarkable property of these waves is that they essentially possess a support that consists of just a few lattice sites [12], providing perhaps the closest experimentally tractable application of the notion of "compactons" [30,31] and establishing the potential for the design and creation of systems with unprecedented properties.

Our concern in this paper, which provides a detailed and expanded description of work we reported in a recent letter [32], is to extend the established theory for uniform granular lattices to nonuniform ones. One way to do this is to study the effects of defects, such as inhomogeneities, particles with different masses, and so on. This has led to the observation of interesting physical responses such as fragmentation, anomalous reflections, and energy trapping [18–26]. In the present paper, on the other hand, we examine the prototypical heterogeneities of granular chains of "dimers" and "trimers," consisting of repetitions of multiparticle cells composed, respectively, of two and three different types of beads. Each lattice "cell," which refers to the fundamental unit of particles that is repeated periodically to form the chain, consists of a single dimer or trimer (e.g., the dimer cell in Fig. 1 consists of N_1 steel beads followed by N_2 polytetrafluoroethylene beads). Such heterogeneities arise in a diverse array of physical settings, including ferroelectric perovskites [33,34] and polymers [35], optical waveguides [36,37], and cantilever arrays [38]. In our granular setting, we use a variety of soft, hard, heavy, and light materials to investigate the effects of different structural properties in the fundamental components of such systems. We also vary the number of beads of a given type in each cell in order to examine the effects of different unit cell sizes (i.e., different periodicities).

More specifically, we investigate solitary wave propagation using experiments, numerical simulations, and theoretical analysis. We report very good agreement between experiments and numerics. For the case of dimer chains, we also construct a long-wavelength approximation to the nonlinear lattice model to obtain a quasi-continuum nonlinear partial differential equation (PDE) that provides an averaged description of the system. We obtain analytical expressions for wave solutions of this equation and find good qualitative agreement between the width and propagation speed of these solutions with those obtained from experiments and numerical simulations.

The rest of this paper is organized as follows. First, we present our experimental and numerical setups. We then consider chains of dimers and discuss our experimental and numerical results. We subsequently use a long-wavelength approximation to derive a nonlinear PDE describing the dimer setup in the case of general power-law interactions between materials and construct analytical expressions for the propagation speed, width, and functional form of its solitary wave solutions. We then compare this continuum theory to our experiments and numerical simulations of the discrete system. Finally, we discuss our experiments and numerical simulations for chains of trimers and summarize our results.

2. Experimental setup

The experimental dimer and trimer chains were composed of vertically-aligned beads in a delrin guide that contained slots for sensor connections or in a guide composed of four vertical garolite rods arranged in a square configuration (see Fig. 1(a)). Each "N_1:N_2 dimer" consisted of a variable number $N_1 \in \{1, \ldots, 7\}$ of one type of bead alternating with $N_2 \in \{1, \ldots, 7\}$ of a second type of bead in a periodic sequence. The "N_1:N_2:N_3 trimers" we studied are defined analogously. The predominant class of configurations we considered included N_1 high-modulus, large mass stainless steel beads (non-magnetic, 316 type) and N_2 low-modulus, small mass polytetrafluoroethylene (PTFE) or Neoprene rubber elastomer beads. We also examined steel:brass, PTFE:glass, and PTFE:nylon dimers and 1:1:1 trimers of steel:brass:PTFE, steel:glass:nylon, and steel:PTFE:rubber. The diameter of all spheres was 4.76 mm.

For each experiment, we connected four calibrated piezosensors to a Tektronix oscilloscope (TDK2024) to detect force–time curves. Three of the piezo-sensors were embedded inside particles in the chain and a fourth one was positioned at the bottom (i.e., at the wall). To fabricate the sensors, beads selected from the various materials were cut into two halves, and slots for sensors and wires were carved within them. Vertically poled lead zirconate titanate piezo elements (square plates with 0.5 mm thicknesses and 3 mm sides), supplied by Piezo Systems, Inc. (RC $= 10^3$ μs), were soldered to custom micro-miniature wires and glued between the two bead halves (see Fig. 1(b)). We calibrated the setup using conservation of momentum. Waves were generated in the chains by dropping a striker from various heights. In most of our experiments, the striker consisted of a stainless steel bead; for some configurations, we also used a PTFE bead, a glass bead, and a PTFE:glass dimer. The material properties for the various beads are shown in Table 1. In our experimental setup, we can measure force amplitude as a function of time in selected particles.[1]

3. Numerical simulations

We model a chain of n spherical beads as a 1D lattice with Hertzian interactions between beads [12,13]:

[1] It is not possible (a priori and without additional assumptions) to infer the nature of kinetic and potential energy distributions as a function of space and time, although clearly this would be interesting because it would allow an in-depth examination and comparison with experiments of theoretical results such as those in Ref. [51].

Table 1
Material properties (mass, elastic modulus E, and Poisson ratio ν) for stainless steel [39,40], PTFE [16,41,42], rubber (McMaster-Carr) [43], brass [44,45], glass [46], and nylon [47]. The value of the dynamic elastic modulus of the rubber beads was extrapolated from the experimental data.

Material	Mass (g)	E	ν
Steel	0.45	193 GPa	0.3
PTFE	0.123	1.46 GPa	0.46
Rubber	0.08	30 MPa	0.49
Brass	0.48	103 GPa	0.34
Glass	0.137	62 GPa	0.2
Nylon	0.0612	3.55 GPa	0.4

$$\ddot{y}_j = \frac{A_{j-1,j}}{m_j}\delta_j^{3/2} - \frac{A_{j,j+1}}{m_j}\delta_{j+1}^{3/2} + g,$$
$$A_{j,j+1} = \frac{4E_jE_{j+1}\left(\frac{R_jR_{j+1}}{R_j+R_{j+1}}\right)^{1/2}}{3\left[E_{j+1}\left(1-\nu_j^2\right)+E_j\left(1-\nu_{j+1}^2\right)\right]}, \quad (1)$$

where $j \in \{1,\ldots,n\}$, y_j is the coordinate of the center of the jth particle, $\delta_j \equiv \max\{y_{j-1}-y_j, 0\}$ for $j \in \{2,\ldots,n\}$, $\delta_1 \equiv 0$, $\delta_{n+1} \equiv \max\{y_n, 0\}$, g is the gravitational acceleration, E_j is the Young's (elastic) modulus of the jth bead, ν_j is its Poisson ratio, m_j is its mass, and R_j is its radius. The particle $j = 0$ represents the striker, and the $(n+1)$st particle represents the wall (i.e., an infinite-radius particle that cannot be displaced). Our numerical simulations incorporate the nonuniform gravitational preload due to the vertical orientation of the chains in experiments but do not take dissipation into account.

The initial velocity of the striker is provided by experimental measurements, and all other particles start at rest in their equilibrium positions, which are determined by solving a statics problem ($\ddot{y}_j = 0$ for all j). Each bead experiences a force from gravity (one can also include a constant precompression f_j, but that is zero for the problem we study). One starts by considering the bottom of the chain with particle n against the wall. It experiences a force F_1 from the top that is the sum of all the forces acting through the center of particle n and a force F_2 from the wall (particle $n+1$) acting through the nonlinear spring (the Hertzian interaction). The expressions for F_1 and F_2,

$$F_1 = \sum_{j=1}^{n} m_j g,$$
$$F_2 = m_n A_{n,n+1}(u_n - u_{n+1})^{3/2}, \quad (2)$$

must be equal at equilibrium. The displacement of the wall $u_{n+1} = 0$ is known, so Eq. (2) and the analogous equation for general k can be solved for the equilibrium displacement of the kth particle ($k \in \{1,\ldots,n\}$) in terms of known quantities:

$$u_k = \left(\frac{\sum_{j=1}^{k} m_j g}{A_{k,k+1}}\right)^{2/3} + u_{k+1}. \quad (3)$$

One applies Eq. (3) to one particle at a time (from the bottom of the chain to the top) to obtain all of the equilibrium positions.

4. Chains of dimers

Let us first discuss our results for chains of dimers. While we focus our presentation on steel:PTFE dimers, we also investigated steel:rubber, steel:brass, PTFE:glass, and PTFE:nylon dimers. Additionally, our presentation includes discussions of 1:1, N_1:1, and 1:N_2 dimers. To compare numerical simulations with experiments, for which the sensors are inserted inside the beads rather than at the points of contact (see panel (b) of Fig. 1), we averaged the force between adjacent beads, $F = (F_j + F_{j+1})/2$, as discussed in detail in Ref. [16]. To show the results of our numerical simulations for the jth bead, we thus plot the force $A_{j-1,j}\delta_j^{3/2} - A_{j,j+1}\delta_{j+1}^{3/2}$ as a function of time.

Our numerical and experimental results greatly expand the previous work reported for chains of dimers composed of particles with similar elastic moduli and different masses [12]. For example, we include investigations of dimers composed of particles with moduli of different orders of magnitude. We also study dimers composed of different numbers of particles (N_1:1 and 1:N_2 chains), thereby varying the "thickness" of the heterogeneous layers.

4.1. 1:1 Dimers

We begin by discussing our results for 1:1 dimers. In Fig. 2, we show experimental and numerical results for 1:1 dimers of steel:PTFE [panels (a, b)] and steel:rubber [panels (c, d)] particles. The steel:PTFE chain consisted of 38 beads, and the steel:rubber chain had 19 beads; in each case, we used a steel bead as the striker. The dynamics indicate that the initial excited impulse develops into a solitary wave within the first 10 particles of the chain. Observe in the steel:PTFE numerics the presence of small-period oscillations after the large solitary pulse. These arise as residual "radiation" emitted by the tail of the wave as it attempts to progress through the highly nonlinear lattice. This is reminiscent of radiative phenomena in different classes of nonlinear lattices, as discussed, for example, in Ref. [48].

Interestingly, even the chains composed of alternating steel and Neoprene rubber beads (inherently nonlinear elastic components) support the formation of solitary-like pulses. However, this configuration is highly dissipative and the solitary waves are consequently short-lived (although this feature is not incorporated in the theoretical model considered herein). As shown in Fig. 2(c, d), the initially very short pulse is quickly transformed into a much wider and slower pulse compared to the dimer composed of steel and PTFE particles. Additionally, the presence of dissipation in the steel:rubber configuration tends to dampen the propagation of the pulses after the first 15 beads. Incorporating dissipative effects is a natural direction for the refinement of the model [49].

To illustrate the robustness of solitary-wave formation, we also studied dimer chains composed of other types of materials, including steel:brass (38 total particles), PTFE:glass (34 particles), and PTFE:nylon (33 particles) configurations. Two important properties of the pulses observed in these systems are their propagation speeds and widths (measured by the full width at half maximum, or FWHM). We compute the pulse speed using time-of-flight measurements for both experiments and computations. To do this, we first measure the peak force of the pulse at each bead and determine the times at which these peaks occur. We then estimate the velocity of the pulse at each bead by examining how long it takes for the pulse (as measured at the peak time) to travel from an earlier bead to a later one. For the numerical calculations, we use the same bead separation distance as in corresponding experiments. For example, for the 1:1 steel:PTFE dimer chain experiments, we measured forces at the beads in positions 13 and 24, so in the numerics we use time-of-flight measurements with an interval of 11 beads.

We depict the results for steel:brass in Fig. 3(a, b) and for PTFE:glass in Fig. 3(c, d). The steel:brass dimer chain included 38 total particles; its striker was a steel bead, which was dropped from about 9.5 cm. We investigated this chain in order to examine a configuration with two different types of large-mass materials with relatively large elastic moduli. It is evident from both experiments and numerical simulations that the system supports the formation and propagation of highly nonlinear solitary waves. These waves have a pulse speed, as measured by time of flight between the first and second sensors, of 499 m/s experimentally and 588 m/s numerically. Their FWHM was measured at 2.0

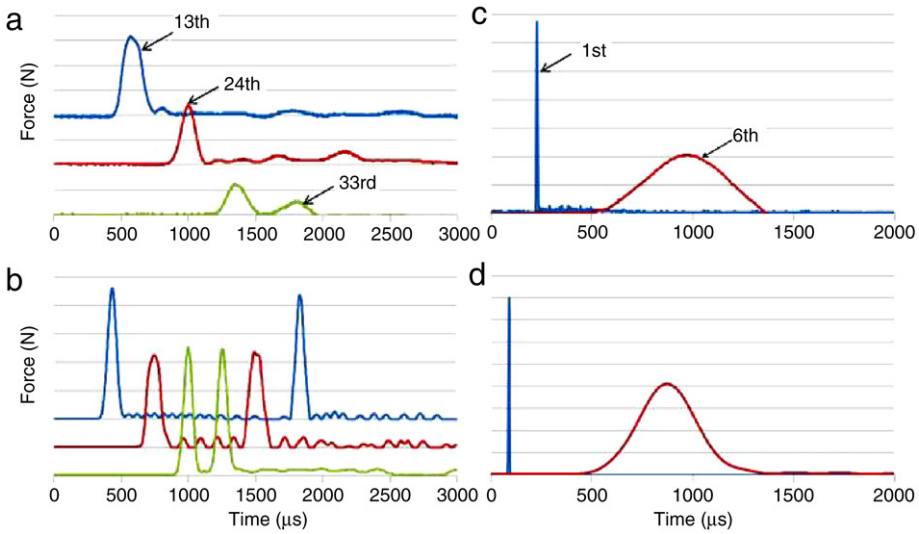

Fig. 2. (Color online) Force versus time response obtained from chains of dimers consisting of 1 stainless steel bead alternating with (a, b) 1 PTFE or (c, d) 1 rubber bead. Panels (a, c) show experimental results, and (b, d) show the corresponding numerical data. For both configurations, the initial velocity of the striker was 1.37 m/s on impact. The *y*-axis scale is 2 N per division in (a, b) and 20 N per division in (c, d). The numbered arrows point to the corresponding particles in the chain. In (a, b), the second curve (showing the results for particle 24) represents a PTFE bead and the other curves represent steel beads. In (c, d), particle 1 is steel and particle 6 is rubber. The force on the rubber particle is magnified by a factor of 20 for clarity.

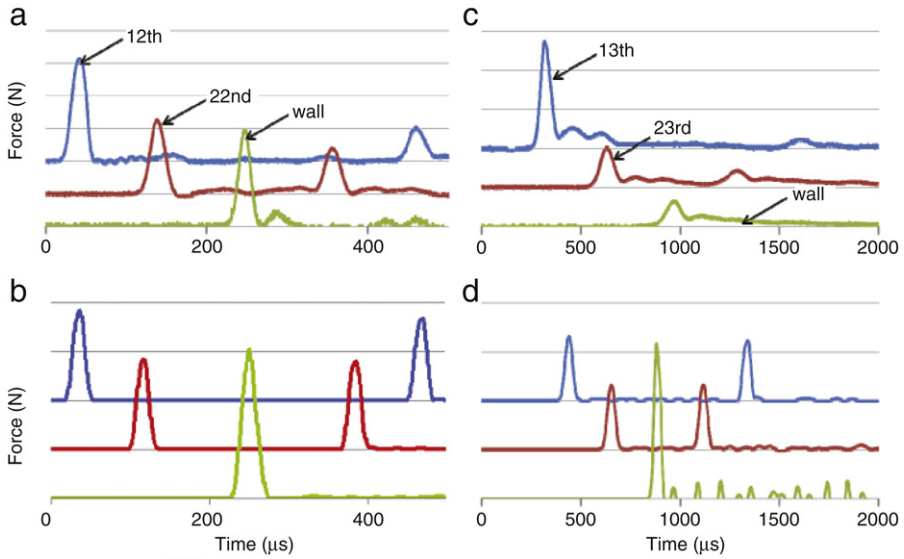

Fig. 3. (Color online) Force versus time response obtained from chains of dimers consisting of (a, b) 1 steel bead alternating with 1 brass bead and (c, d) 1 PTFE bead alternating with 1 glass bead. Panels (a, c) show experimental results, and (b, d) show the corresponding numerical data. The numbered arrows point to the corresponding particles in the chains. For the steel:brass configuration, a steel striker impacted the chain with an initial velocity of 1.21 m/s. The *y*-axis scale is 5 N per division in (a) and 20 N per division in (b). For the PTFE:glass configuration, a glass striker impacted the chain with an initial velocity of 1.17 m/s. The *y*-axis scale is 1 N per division in (c) and 3 N per division in (d).

beads (1.0 cells) and 2.1 beads (1.05 cells) in experiments and numerics, respectively. PTFE:glass dimer chains provide another configuration consisting of two different particles with similar masses, but in this case the masses are smaller than with steel:brass and the elastic moduli and (especially) Poisson ratios of the two materials are rather different. Although it is composed of lighter and softer particles, this dimer chain nevertheless supports the formation and propagation of solitary-like pulses. The signal speed is significantly reduced (it is 152 m/s in experiments and 221 m/s in the numerics), and the pulse FWHM is 2.0 beads (1.0 cells) experimentally and 2.1 beads (1.05 cells) numerically. In addition, secondary oscillations can be observed both in experiments and (to a lesser extent) in numerical simulations [see, in particular, the bottom (wall) signal in Fig. 3(d)]. Finally, the PTFE:nylon chain (with a PTFE striker dropped from a height of 2.5 cm) provides a configuration with one small mass and a second mass that is extremely small. Unlike rubber, the nylon beads do not lead to severe dissipation. However, this configuration appears to have greater difficulty in forming and supporting solitary waves, at least in the chain lengths studied (33 beads).

As we have suggested, dimer chains have decidedly different properties from uniform chains. We find numerically that the solitary pulse in uniform chains has an FWHM of about 2.1 cells (i.e., 2.1 beads), consistent with prior observations (see, e.g., Fig. 1.4 in [12]). Because of the similar masses in the steel:brass and PTFE:glass chains, the pulse width in those 1:1 dimer chains is similar to that obtained for uniform chains. We observe this feature both experimentally and numerically. (As discussed later,

Fig. 4. (Color online) Force versus time response obtained from chains of dimers consisting of (a, b) 2 and (c, d) 5 stainless steel beads alternating with 1 PTFE bead. The total number of beads is 38 in each case. Panels (a, c) show experimental results, and (b, d) show the corresponding numerical data. For both experimental configurations, the striker had an impact velocity of 1.37 m/s with the chain. The y-axis scale is 2 N per division for (a, c) and 1 N per division for (b, d). The numbered arrows point to the corresponding particles in the chain. For both configurations, the second curve (showing the results for particle 24) represents a PTFE bead and the other curves represent steel beads.

the theoretical prediction for the mean FWHM in dimer chains depends only on the mass ratio of the two bead materials because the elastic modulus and Poisson ratio can both be scaled out; future studies will address the effects of changing E and ν. The existence of the dimer is built into the long-wavelength asymptotics used to derive this result.) This suggests that there is a "critical" mass ratio m_1/m_2 necessary for the system to become "sensitive" to the existence of the dimer. This poses an interesting question concerning what is the critical point (mass ratio) for the dynamics to resemble that of a chain with periodic "defects." That is, how large (or small) should m_2 be to obtain bona fide dimer dynamics (increased pulse width, etc.)?

In the case of homogeneous chains, asymptotic analysis predicts a wave width of about 5 cells from tail to tail [12]. The propagation speed of the pulses in steel is quite large; for steel strikers with an impact velocity of 1.37 m/s, we found numerically that the pulse propagates at almost 700 m/s, and other authors have found large experimental propagation speeds with other initial conditions [47]. In contrast, as discussed in detail below, pulses in dimers have a shorter width in terms of number of cells. With a steel striker with a velocity of 1.37 m/s on impact, we find for 1:1 steel:PTFE dimer chains a propagation speed of 168 m/s numerically and 128 m/s experimentally. In Section 4.3, we present an asymptotic analysis of the width of highly nonlinear solitary waves in 1:1 dimer chains, which we compare to the previously-studied limiting cases of monomer chains and 1:1 dimers with beads of mass m_1 and $m_2 \ll m_1$ [12]. Preliminary experiments and numerical simulations on 1:1 dimers, considering only materials with elastic moduli of the same order of magnitude (and mass ratios m_1/m_2 of 2, 4, 16, 24, and 64), are described in Ref. [12].

4.2. N_1:1 and 1:N_2 dimers

We consider configurations with different periodicities by varying the number of steel and PTFE particles in steel:PTFE dimers. We obtain robust pulses for N_1:1 dimers with $N_1 > 1$ (with N_1 as high as 7 in experiments and as high as 22 in numerics), though the transient dynamics and spatial widths of the developed solitary-like waves are different. This is clearly illustrated in Fig. 4 through experimental and numerical results for 2:1 and 5:1 steel:PTFE dimers. The difference in transient dynamics can be intuitively understood in terms of the increasing difficulty of the system in forming a single solitary pulse as N_1 increases (due to the presence of the 1 bead of different type in each cell of an otherwise uniform chain). On the other hand, the spatial widths differ through a mechanism similar to the one that we will explain analytically (see the discussion below) for the 1:1 configurations. Each bead in a given cell (i.e., each instance of the dimer) responds differently but consistently throughout the chain. For example, in the 2:1 chain, the second steel bead in a cell possesses a cleaner and more solitary-like shape than the first or third bead. This is especially evident in the numerical simulations.

For the 5:1 dimers, there is a critical length scale difference between the pulse size one would obtain in a uniform chain of beads (for which the predicted width is about 5 particles long [12]) versus the pulse size one would obtain in a 5:1 chain (about 30, corresponding to the presence of 5 unit cells with 6 particles each). The observed pulse width encompasses a smaller number of cells than for 1:1 dimers. More generally, we observed both numerically and experimentally that the width (in terms of the number of cells) of the solitary waves decreases gradually with increasing numbers N_1 of steel beads in a single dimer (cell) from the 5-cell width expected for Hertzian interactions. It takes roughly six cells to achieve a stable pulse for the 2:1 configuration, whereas it takes 12 cells for the 5:1 configuration. (It also takes roughly 6 cells for the pulse in the 3:1 chain to stabilize and roughly 11 cells for that in the 4:1 chain to stabilize.) This difficulty in creating a "clean" and stationary solitary pulse reflects the increased difficulties in considering an N_1:1 cell as a "quasiparticle" as N_1 increases.

We observe in our experiments that the width of the solitary waves (in terms of the total number of cells) decreases with N_1, although the number of "participating" beads increases with N_1. For the numerics, the FWHM seems to be steady at first, but it is smaller for $N_1 = 4$ as the aforementioned length scale difference arises. We observe that the pulse speed increases with increasing N_1 in both experiments and numerics. This is physically justified because the increase in the number of steel particles makes the system generally "stiffer." For each configuration, the scaling between the pulse's maximum force and its speed of propagation